Dictyostelium Mutants Lacking the Cytoskeletal Protein Coronin Are Defective in Cytokinesis and Cell Motility

Eugenio L. de Hostos, Christoph Rehfueß, Birgit Bradtke, David R. Waddell, Richard Albrecht, John Murphy, and Günther Gerisch

Max-Planck-Institut für Biochemie, 8033 Martinsried, Germany

Abstract. Coronin is an actin-binding protein in *Dictyostelium discoideum* that is enriched at the leading edge of the cells and in projections of the cell surface called crowns. The polypeptide sequence of coronin is distinguished by its similarities to the β-subunits of trimeric G proteins (E. L. de Hostos, B. Bradtke, F. Lottspeich, R. Guggenheim, and G. Gerisch. 1991. *EMBO (Eur. Mol. Biol. Organ.) J.* 10:4097–4104). To elucidate the in vivo function of coronin, null mutants have been generated by gene replacement. The mutant cells lacking coronin grow and migrate more slowly than wild-type cells. When these *cor*⁻ cells grow in liquid medium they become multinucleate, indicating a role of coronin in cytokinesis. To explore this role, coronin has been localized in mitotic wild-type cells by immunofluorescence labeling. During separation of the daughter cells, coronin is strongly accumulated at their distal portions including the leading edges. This contrasts with the localization of myosin II in the cleavage furrow and suggests that coronin functions independently of the conventional myosin in facilitating cytokinesis.

A variety of proteins that interact with actin have been shown in vitro to perform functions which are conceivably necessary to make actin play its diverse roles in non-muscle cells: motor proteins, cross-linking factors, severing, capping, and membrane anchoring proteins (Pollard and Cooper, 1986). Genetic approaches to identify in vivo functions directly have been concentrated on a few eukaryotic organisms or cell types (for reviews see Gerisch et al. 1991, and Noegel and Schleicher, 1991; Cunningham et al., 1991, 1992). One of the organisms investigated is *Dictyostelium discoideum.* In this microorganism the actin system is involved in cell motility, cytokinesis and multicellular development (for reviews see Devreotes and Zigmond, 1988; Schleicher and Noegel, 1992).

Dictyostelium mutants that are defective in the production of myosin II heavy chains have shown that the interaction of myosin II with actin plays a role in cytokinesis, ameboid locomotion, intracellular particle movement, and in the capping of cell-surface proteins (Knecht and Loomis, 1987; De Lozanne and Spudich, 1987; Wessels et al., 1988; Manstein et al., 1989; Fukui et al., 1990; Wessels and Soll, 1990; Jay and Elson, 1992). Furthermore, the fact that motility and chemotactic orientation is reduced but not abolished in the myosin II–defective cells has established the importance of other proteins, probably members of the myosin I family (Titus et al., 1989; Jung and Hammer, 1990).

Efforts to correlate the in vitro effects of actin-binding proteins with their roles in vivo have not always led to such straightforward results, however. Examples that emphasize these difficulties are three other cytoskeletal proteins in *Dictyostelium* that either cross-link or sever actin filaments. In vitro, α-actinin and the 120-kD gelation factor (ABP-120) are the most active cross-linking proteins as revealed by viscometry. Their elimination, however, has resulted only in weak (Wallraff et al., 1986; Brink et al., 1990) or moderate (Cox et al., 1992) changes of cell behavior, and all mutants lacking one of these proteins proceed in multicellular development up to the final stage of fruiting body formation. In part, this appears to be due to an overlap in function of the two cross-linking proteins: double mutants that lack both of them move and chemotax but exhibit difficulties in developing beyond the aggregation stage (Witke et al., 1992). A third actin-binding protein eliminated in *Dictyostelium* is severin, a homolog of vertebrate gelsolin. Although, in the presence of Ca^{2+}, severin is the most active actin fragmenting protein in *Dictyostelium* as judged by in vitro assays, its elimination causes no substantial alterations of cell behavior and development (André et al., 1989).

These findings showing that proteins with strong activities in vitro may be eliminated without severe consequences to the cells, have prompted us to search for new actin-binding proteins independently of their activities in vitro. The goal has been to identify those proteins still present in the α-actinin, ABP120 and severin defective mutants that enable the cells to regulate chemotaxis and to perform other actin-based activities. One approach has been to characterize pro-

Dr. de Hostos' present address is Department of Pharmacology, University of California, San Francisco, CA 94143-0001.

Dr. Waddell's current address is Department of Biological Sciences, Beloit College, Beloit, WI 53511.

teins that coprecipitate with reconstituted actin-myosin complexes. One of these proteins, coronin, turned out to be of particular interest because of its sequence relationships to the β-subunits of trimeric G proteins, and because of its localization to crown-shaped surface extensions and to the leading edges of moving cells (de Hostos et al., 1991). In the present paper we show by gene replacement that coronin has important functions in cell motility and cytokinesis.

Materials and Methods

Strains

The axenic AX2-214 strain of *D. discoideum* is referred to as wild type. The locus encoding coronin has been designated as *cor*, and mutants lacking coronin are referred to as *cor*$^-$. Four coronin mutant strains have been characterized and designated as HG1568, HG1569, HG1570, and HG1571.

Culture Conditions

Cells were cultivated at 23°C under various conditions. The cells were grown axenically in nutrient medium (Ashworth and Watts, 1970) as specified by Claviez et al. (1982) either in suspension, or on the bottom of a plastic culture dish overlaid with medium. For some experiments cells were grown on coverslips placed on the bottom of the dish. For growth on bacteria cells were cultivated on SM nutrient agar plates in lawns of *Klebsiella aerogenes*.

Coronin Gene Replacement

The gene replacement strategy was based on that of Manstein et al. (1989). The construct consisted of three fragments, corA and corB, derived from coronin cDNAs, and a G418^r cassette conferring resistance to the antibiotic G418 (see Fig. 1). CorA was derived from a cDNA fragment encoding the amino-terminal two-thirds of coronin cloned into pUC19. The fragment was modified by destroying its unique PstI restriction site and was then used as a substrate for the amplification of corA by polymerase chain reaction (PCR)[1] using primers which incorporated unique SphI (primer A5′) and XbaI (A3′) sites into the amplified product. CorB, a fragment encoding the carboxy-terminal one-third of coronin, was derived by PCR from a full-length coronin cDNA originally derived by PCR from a λ-gt11 phage (de Hostos et al., 1991). The primers used incorporated unique XbaI (B5′) and SacI (B3′) sites into the amplified product. The oligonucleotide primers used had the following sequences:

A5′:5′gcttgcatgcgatgtctaaagtagtccg3′;
A3′:5′cgactctagagatagagtttgttcttgg3′;
B5′:5′cgactctagacgtttgtcaccaaggtgtc3′;
B3′:5′taccgagctcgagttctttgattttggc3′.

The G418^r cassette was isolated as an XbaI–XbaI fragment, subcloned from the vector pDNeoII (Witke et al., 1987). The cassette consists of the neomycin-phosphotransferase gene from Tn903 cloned between the promoter and terminator sequences of the *Dictyostelium* actin-15 gene (Knecht et al., 1986).

The gene replacement construct was assembled in two steps. First, corA digested with SphI and XbaI, corB digested with SacI and XbaI, and vector digested with SphI and SacI were ligated and introduced into *Escherichia coli* JM105. Finally, the corA-corB plasmid was digested with XbaI and ligated with the XbaI-XbaI G418^r fragment and cloned. The orientation of the antibiotic resistance cassette relative to the coronin sequences was not determined in the final construct. A large-scale preparation of the gene replacement construct was carried out using a Quiagen column (Diagen, Düsseldorf, Germany).

For transformation, 15 μg of the plasmid carrying the gene replacement construct were digested with SphI and SacI, dephosphorylated using calf intestinal phosphatase at 57°C, precipitated, and resuspended in 10 μl electroporation buffer (50 mM sucrose, 10 mM K-phosphate, pH 6.1, sterilized by filtration).

For electroporation, AX2 cells were grown axenically in suspension culture to a density of 2–3 × 10^6 cells/ml and then chilled on ice and washed in ice-cold 17 mM Na/K-phosphate buffer, pH 6.0 (PB). The cells were then washed once more and resuspended in electroporation buffer at a concentration of 1 × 10^8 cells/ml. DNA was mixed with 500 μl of cell suspension and the mixture was transferred to a chilled cuvette (2-mm gap) and electroporated with the Bio-Rad Gene Pulser set at 1 kV and 3 μF, without the pulse controller.

After poration the cells were transferred to a culture dish and incubated at room temperature for 10 min. Then 100 mM $CaCl_2$ and $MgCl_2$ were added to a final concentration of 1 mM each and the cells were shaken gently for 15 min at 23°C. The cells were resuspended in 100 ml of medium and distributed into five culture plates. The plates were incubated 24 h before changing the medium and adding 6 μg/ml of G418 (Geneticin; Sigma Chemical Co., St. Louis, MO). The G418 concentration was increased to 10 and finally to 12.5 μg/ml over the following 3 d. Colonies were picked with a pipetter and transferred to culture dishes for subcloning. Except in experiments to test for reversion, 1% penicillin/streptomycin antibiotic stock solution for tissue culture (Gibco-BRL, Gaithersburg, MD) and G418 were added to axenic cultures of transformants.

Antibody Blots

Total cellular proteins were resolved by SDS-PAGE in 13% gels (Laemmli, 1970), transferred to nitrocellulose in a semi-dry blotting device and then incubated with a mixture of culture supernatants from hybridoma cell lines 176-3-6 and 176-2-5 obtained as described by de Hostos et al. (1991). After incubation with phosphatase-conjugated goat-anti-mouse antibody (Dianova, Hamburg, Germany) the blots were developed using 5-bromo-4-chloro-3-indolylphosphate (Sigma Chemical Co.) as a substrate and nitro blue tetrazolium (Sigma Chemical Co.) as an enhancer in buffer containing 100 mM NaCl, 5 mM $MgCl_2$, 100 mM Tris-Cl, pH 9.5 (Harlow and Lane, 1988).

Colony blots were prepared as described (Wallraff et al., 1986). After staining with Ponceau S (Sigma Chemical Co.) the blots were placed in boiling SDS-PAGE running buffer for one min to denature the proteins and render any coronin present detectable by the antibody. The blots were incubated with radioiodinated mAb 176-3-6.

Fluorescence Microscopy

For synchronization of cell division, cells were washed in PB at the end of the log phase (~7 × 10^6 cells/ml), resuspended at a concentration of ~2 × 10^6 cells/ml, and shaken at 4°C for 12–24 h. Drops were placed on acid-cleaned glass coverslips in a culture dish. After allowing the cells to settle down for 15 min the plates were filled with nutrient medium and incubated at 23°C. The cells were fixed when signs of mitotic activity were observed, usually after 4 h in medium.

Unless otherwise indicated, the cells for fluorescence microscopy were fixed with picric acid/paraformaldehyde, labeled, and mounted as described (Bomblies et al., 1990; de Hostos et al., 1991). Coronin was localized using mAb 176-3-6 (de Hostos et al., 1991). The mAb was labeled with FITC and TRITC-labeled goat anti-mouse antibodies (Jackson Immunoresearch, West Grove, PA). F-actin was labeled with TRITC-phalloidin (Sigma Chemical Co.). For the labeling of myosin (see Fig. 8) the cells on coverslips were covered by an agar overlay (Fukui et al., 1987) and then fixed with picric acid/paraformaldehyde. Myosin was labeled with rabbit antibodies against *Dictyostelium* myosin II, kindly provided by Dr. J. Spudich (Stanford University, Stanford, CA) (Berlot et al., 1985), and TRITC-labeled goat anti-rabbit antibodies (Cappel Laboratories, Cochranville, PA). For the nuclear-count experiment the cells were fixed in absolute methanol (−20°C, 15 min), air dried, and then stained 5–10 min with 0.5 μg/ml of 4,6-diamino-2-phenylindole (DAPI; Hoechst) in buffer consisting of 50 mM KH_2PO_4, 2 M NaCl, 20 mM EDTA, pH 7.4. The cells were washed in buffer without DAPI, rinsed in distilled water, mounted, observed in an Axiophot microscope (Carl Zeiss, Oberkochen, Germany), and photographed on Tri-Xpan film (Eastman Kodak Co., Rochester, NY).

Growth Rates

Both mutant and wild-type cells were inoculated at an initial concentration of approximately 5 × 10^5/ml in medium without G418 but containing 1% penicillin/streptomycin. Periodically, aliquots were taken and incubated on ice ≥20 min before counting with a Coulter Counter in Isoton buffer diluted 1:10 with water (Waddell et al., 1987).

1. *Abbreviations used in this paper*: PB, Na/K-phosphate buffer; PCR, polymerase chain reaction.

Scanning EM

Cells grown on coverslips were fixed with drops of chilled PB containing freshly added OsO_4 and glutaraldehyde to final concentrations of 0.02 and 1%, respectively, and left at room temperature for 30 min. After dehydration through an ethanol series (10 min each, 30, 50, 80, and 95%), then 100% ethanol (2 × 10 min) and finally 100% acetone (2 × 10 min), the samples were equilibrated in liquid CO_2 for 30 min before critical point drying. The samples coated with gold were viewed with a Jeol JSM 35C scanning electron microscope (JSM 35C; JEOL USA, Peabody, MA).

Chemotaxis

Motility assays and chemotaxis experiments were performed essentially as described by Fisher et al. (1989). Cells grown in axenic suspension culture to a density of ~5 × 10^6 cells/ml were washed, resuspended, and shaken in PB at a density of 1 × 10^7 cells/ml for 6 h before transfer to a chemotaxis chamber in which a stable cAMP gradient could be established. The movements of the cells were observed using a Zeiss Axiomat inverted microscope equipped with a video camera (TV-11-35 High Resolution Camera, VTE Digitalvideo, Herrsching, Germany), and analyzed by a PC containing a 486 CPU, that hosted an image processing system (Imaging Technologies Inc., Woburn, MA).

The chemotaxis chamber was first perfused with PB for 1 h and the movements of the cells were recorded during the second half-hour period (PB without cAMP gradient). Then a cAMP gradient was established for half an hour (25 nM/mm, midpoint 25 nM) and cell movements were recorded during the next half-hour period, by which time a stable, linear gradient was established.

Images were recorded every 45 s and by digital analysis the following parameters were calculated (Fisher et al., 1981; Fisher et al., 1983; Segall et al., 1987): speed (μm/min), turning rate (radians^2/min), and kappa (κ), an orientation index. The turning rate ranges from zero, for a straight path, to infinity, for a path in which the direction of any movement step is unrelated to any previous one. κ describes the ability of the cells to orient in the cAMP gradient; it ranges from zero, for paths with no orientation, to infinity, for perfectly oriented paths.

Nucleic Acid Hybridization

Genomic DNA prepared as described by Mehdy et al. (1983) was restricted and resolved by electrophoresis through a 0.8% agarose gel. After denaturing the gel was neutralized with 1 M ammonium acetate, and the DNA transferred to nylon membrane (Pall Biodyne, East Hills, NY) in the same buffer overnight and cross-linked to the membrane on a transilluminator for 90 s. A cDNA probe was labeled by the random priming method (Feinberg and Vogelstein, 1983) and hybridized to the filters as described by Mehdy et al. (1983) in buffer containing 45% formamide at 37°C.

For the preparation of RNA, cells grown in suspension culture were washed with PB, resuspended in a buffer containing 1% β-mercaptoethanol, 10% sucrose, 10 mM Mg-acetate, 10 mM NaCl, and 10 mM Hepes, pH 7.5, and lysed by the addition of NP-40 to a final concentration of 2%. The lysate was cleared by centrifugation and the supernatant was mixed with an equal volume of 50 mM Tris-HCl, pH 7.5, containing 2% SDS. After extractions with phenol and chloroform/isoamyl alcohol RNA was precipitated successively with isopropanol and NaCl, 8 M LiCl, and finally with ethanol and Na-acetate. The RNA was resolved by electrophoresis in 1.2% agarose gels containing formaldehyde, transferred to nylon membrane and crosslinked. The blots were hybridized as described by Mehdy et al. (1983) in buffer containing 55% formamide at 37°C.

Results

Generation of Coronin Mutants by Gene Replacement

Dictyostelium cells were transformed with a linear construct (Fig. 1) designed for gene replacement mutagenesis (Manstein et al., 1989; Jung and Hammer, 1990; Cox et al., 1992). Colonies began to appear after a week in axenic medium containing G418, and 40 of them were picked at random and subcloned. Microscopic examination showed that the cells in at least ten of the clones had an unusual appearance (Fig. 2). Many cells were large and had irregular shapes

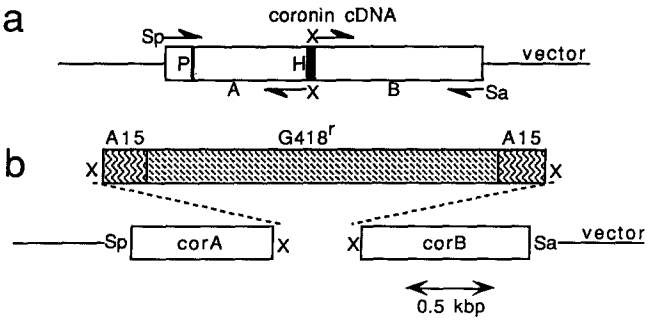

Figure 1. Construction of coronin gene replacement vector. (*a*) Generation of coronin cDNA fragments corA and corB. The bars labeled P and H represent the deletion of PstI and HincII sites, respectively. The arrows represent PCR primers and their letters the restriction sites incorporated into the amplified fragments (*Sp*, SphI; *X*, XbaI; *Sa*, SacI). (*b*) Assembly of the linear gene replacement vector. The corA and corB fragments generated by PCR were ligated together with the antibiotic resistance cassette from the pDNeoII vector. In this cassette the phosphotransferase coding region (*G418r*) is flanked by *Dictyostelium* actin-15 promoter and terminator sequences (*A15*).

with many fronts and numerous vacuoles. In these clones cells of normal size were also present but they seemed to be less well spread and thus more compact in their appearance on a plastic surface. The large cells were multinucleate, as shown by staining with DAPI (Fig. 2). Examination by immunofluorescence microscopy of some of the clones containing large cells showed no labeling of coronin (Fig. 3, *a* and *b*). Thus the tendency to form large cells was accompanied by the absence of the coronin antigen.

Based on their appearance and putative *cor*$^-$ phenotype, four independent transformant clones (strains HG1568, HG1569, HG1570, and HG1571) were chosen for further characterization. A Western blot of total cellular proteins from subcultures of these four strains was incubated with a mixture of two mAbs directed against coronin. No antigen was detectable among the proteins from strains HG1569, HG1570, or HG1571 after axenic growth in medium with or without G418 (Fig. 4 *a*; for the results on strain HG1568 see next section).

When inoculated on a lawn of bacteria, strains HG1569, HG1570, and HG1571 grew at a rate considerably slower than that of the wild-type strain. After two days of growth they had approximately one-half the diameter of the AX2 colonies. However, unlike cells lacking the myosin II heavy chain which are also slow-growing, cells from the *cor*$^-$ strains formed fruiting bodies and sporulated. The *cor*$^-$ cells had a wild-type appearance during growth on bacteria, but when transferred to axenic medium in plastic dishes they regained their large size. In axenic suspension culture, the generation time of the coronin mutants was also longer than that of the parent strain. Whereas the doubling time at 23°C was ~8 h in AX2, it was 13 h in the mutants HG1569 and HG1570. Strain HG1571 grew even more slowly with a doubling time of ~18 h.

In wild-type cells coronin is known to be enriched in extensions of the cell cortex called crowns (de Hostos et al., 1991). The question was therefore whether coronin is essential for the formation of these structures. Phalloidin labeling

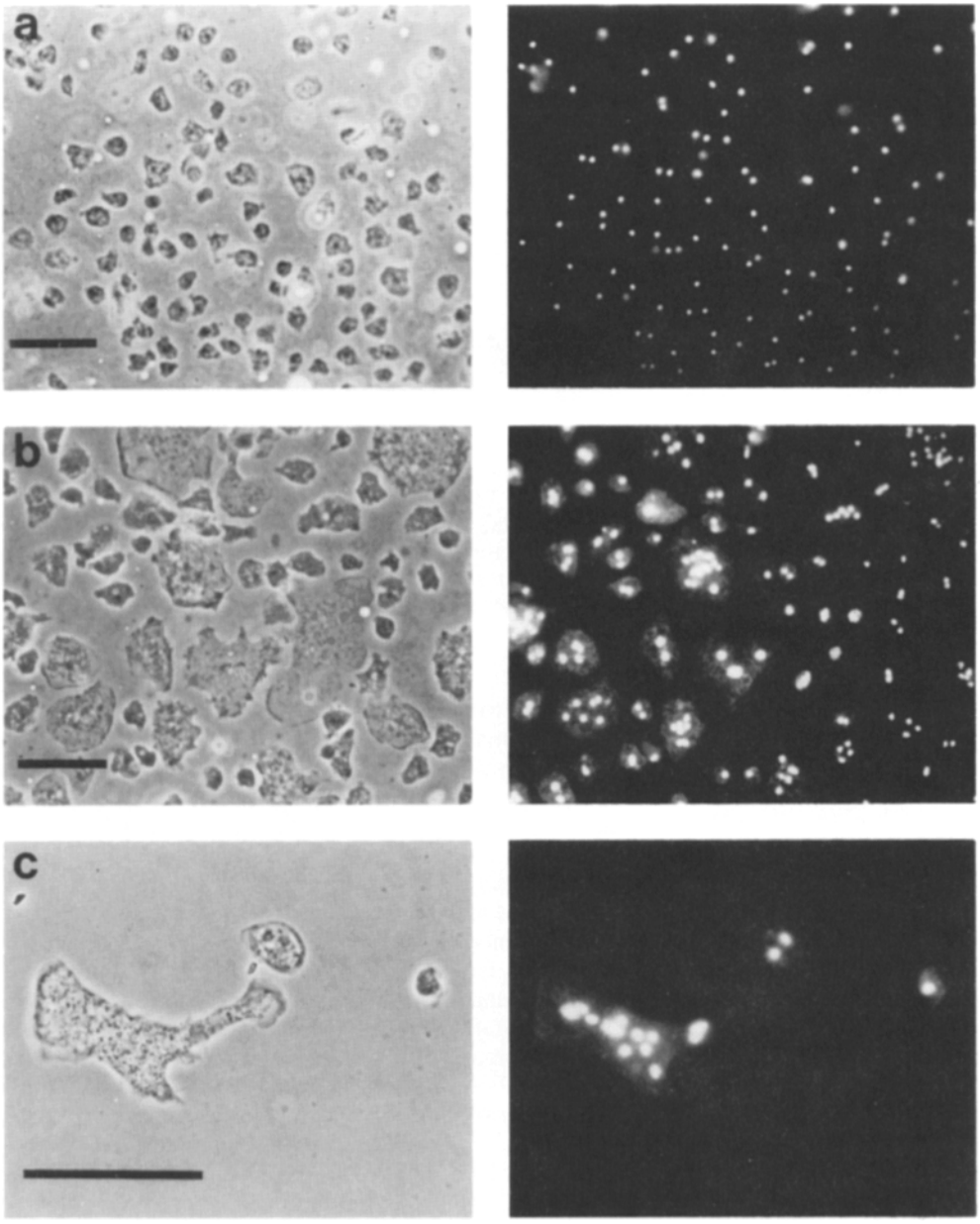

Figure 2. Mostly mononucleate cells in the AX2 wild type (*a*) and abundance of multinucleate cells in the *cor*⁻ mutant HG1569 (*b* and *c*). Left panels show cells viewed by phase contrast microscopy, right panels nuclei of the same cells labeled with DAPI and viewed by fluorescence microscopy. Bars, 50 μm.

revealed a distribution of F-actin in *cor*⁻ cells similar to that seen in the wild type (Fig. 3, *c* and *d*). In both wild-type and mutant cells F-actin was accumulated at the cell periphery, most strongly at the front and in the crowns. Thus the reduction in growth rate is not related in the *cor*⁻ mutants to an obvious alteration in the assembly or localization of actin filaments. Viewing by scanning EM confirmed that the cells have the capacity to build crown-shaped extensions in the absence of coronin (Fig. 5).

Renewed Coronin Expression in an Unstable Mutant Is Accompanied by Reversion to the Wild-type Phenotype

In a Western blot of the lysate from a subculture of the fourth strain analyzed, HG1568, antigen comigrating with wild-type coronin was detectable but in a reduced amount relative to the parent AX2 strain (Fig. 4 *a*). The coronin was detectable in HG1568 after growth with or without G418. The following results showed that this mutant is unstable, and coronin production is due to the presence of revertants.

Among the colonies obtained by recloning of the HG1568 strain on a lawn of bacteria, most grew as slowly as those of the other *cor*⁻ strains, but there were also some colonies or sectors which grew faster. A colony blot incubated with anti-coronin antibody showed that coronin was produced in the faster growing sectors. (Fig. 4, *b* and *c*). Cells isolated from these spots did not regain an unusual appearance after being transferred to axenic medium. Thus in these cells the renewal of coronin expression was accompanied by stable reversion to the wild-type phenotype.

Cor⁻ *Mutants Migrate Slowly but Orient in a cAMP Gradient*

A quantitative evaluation of motility and chemotactic orientation was undertaken using an image analysis system (Fisher et al., 1989). The behavior of aggregation-competent

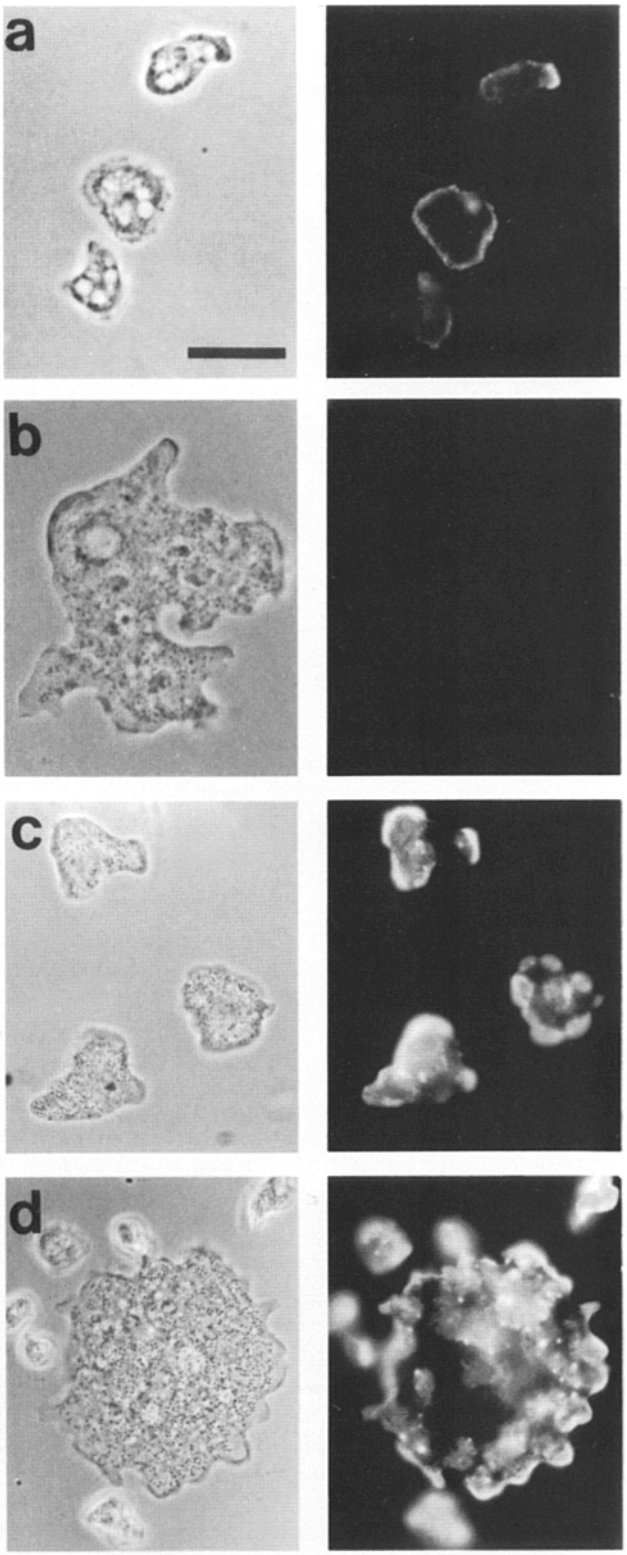

Figure 3. Localization of F-actin in *cor*$^+$ and *cor*$^-$ cells. Micrographs are shown pairwise with the phase contrast image at the left and the fluorescence image on the right. Cells labeled with anti-coronin antibodies: (*a*) control transformant in which no gene disruption has occurred; (*b*) large HG1569 transformant cell with irregular morphology lacking coronin. Cells labeled with phalloidin; (*c*) wild-type cells; (*d*) HG1569 *cor*$^-$ cells. Bar, 15 μm.

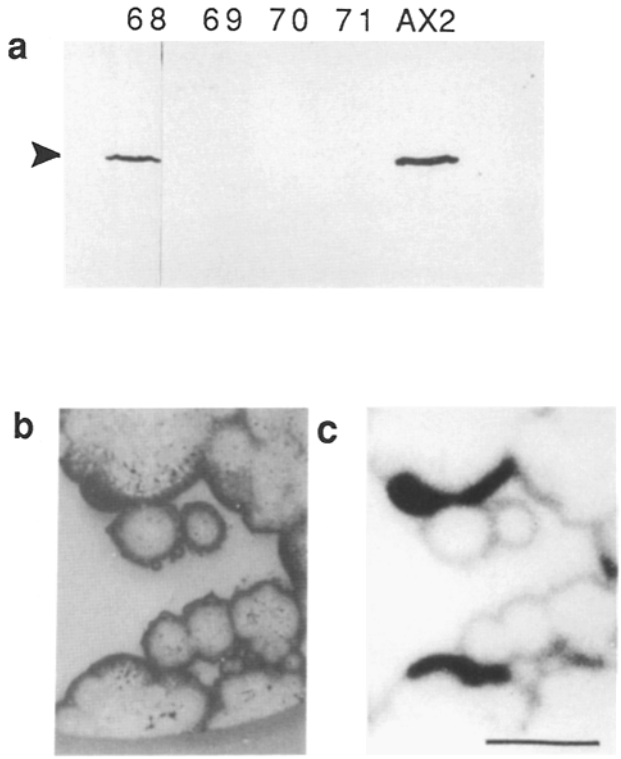

Figure 4. Western blots of wild-type and transformants. (*a*) Total cellular proteins separated by SDS-PAGE, from AX2 cells and from the mutant strains HG1568 (*68*), HG1569 (*69*), HG1570 (*70*), and HG1571 (*71*) after labeling with anti-coronin antibodies. (*b*) Blot of HG1568 colonies stained with *Ponceau S.* (*c*) Autoradiograph of the colony blot shown in *b* after incubation with anti-coronin antibody showing sectors formed by revertants expressing coronin. Bar, 1 cm.

cor$^-$ and wild-type cells was analyzed in buffer without chemoattractant, and in a stationary gradient of cAMP. Table I shows the speed of migration, turning rate, and the chemotactic orientation index κ. The mutant cells migrated at reduced average velocities of 3 μm/min in buffer alone and 5 μm/min in the cAMP gradient, which were about half of the wild-type speeds of 7 and 12 μm/min, respectively. Nevertheless, in the cAMP gradient the *cor*$^-$ cells performed chemotaxis with a moderately reduced precision comparable to the AX2 strain. These results show that the migration of cells lacking coronin was slow but still effectively oriented.

A characteristic feature of *cor*$^-$ cell behavior is the narrow range of velocities of migration. AX2 cells (Fig. 6 *a*) had a typical broad distribution of velocities, whereas the HG1569 cells (Fig. 6 *b*) showed a sharp upper limit of speed. This means that virtually no cells migrated considerably faster than the bulk of the population. The inserts illustrate the differences in *cor*$^-$ and wild-type behavior. The examples show tracks from cells in buffer (left) and in a cAMP gradient (right).

Cor$^-$ *Cells Are Defective in Cytokinesis*

The multinucleate phenotype of the *cor*$^-$ cells grown in axenic culture resembles that of myosin II–defective cells,

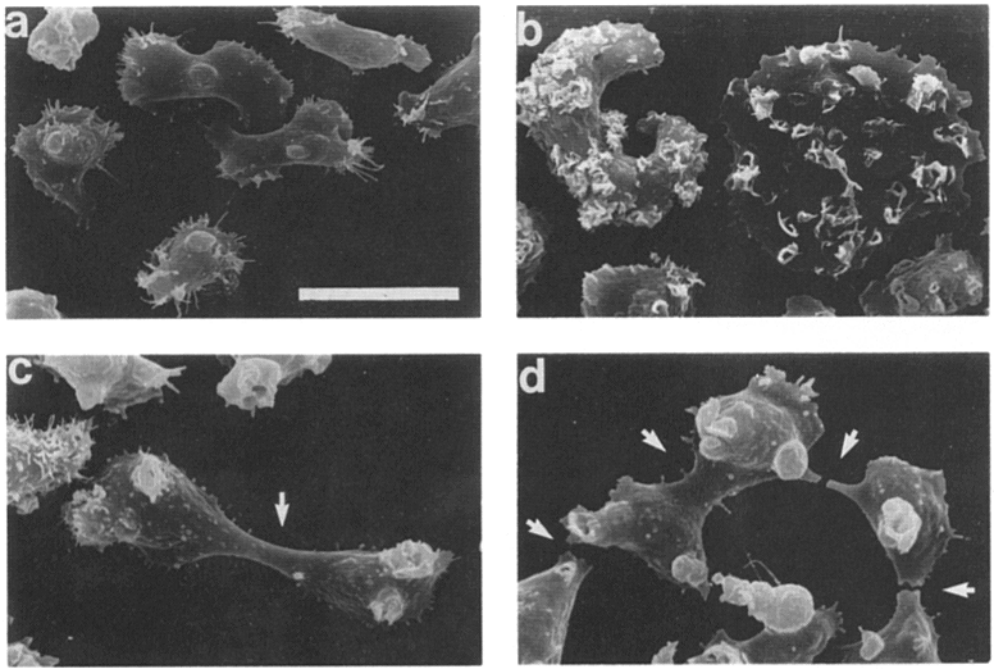

Figure 5. Scanning electron micrographs of wild type and *cor*⁻ cells showing cell shape and surface structures. Both wild type (*a*), HG1568 cells (*b*), and HG1571 cells (*c* and *d*) show crown-shaped surface extensions and filopods. The constrictions indicated by arrows in *c* and *d* may indicate cell division. (The ruptures seen in the cell in *d* are artifacts of specimen drying.) Bar, 15 μm.

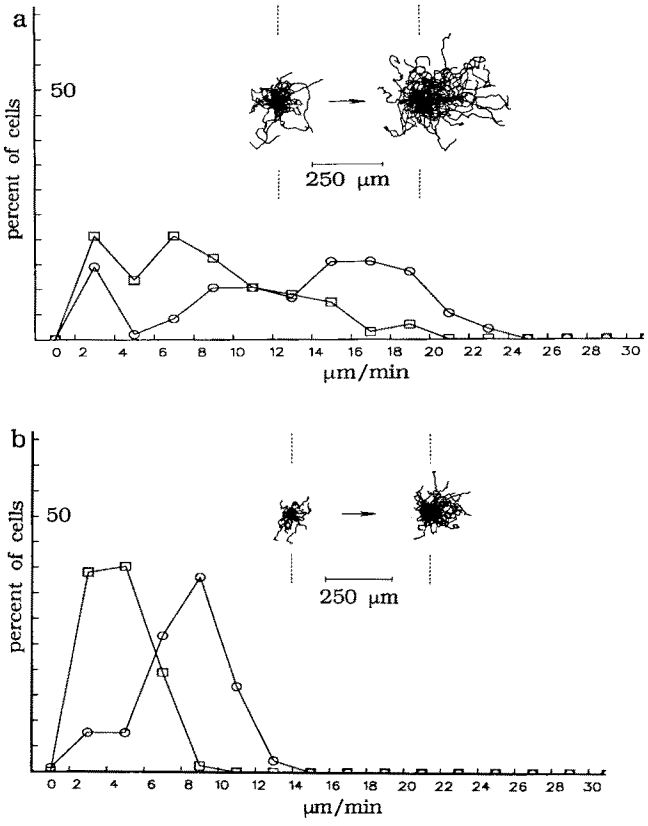

Figure 6. Motion analysis of AX2 cells (*a*) and HG1569 cells (*b*). The histograms show the distribution of speeds of unstimulated cells (□) and of cells exposed to a cAMP gradient (○). The insets show representative migration patterns in wild type and mutant populations of unstimulated cells (pattern on the left) or of cells in a gradient with the high cAMP concentration on the right side (pattern on the right). The tracings of individual cell paths during 30 min of recording have been superimposed and plotted with a common origin. These examples were chosen on the basis of their average speed, which was closest to the mean value obtained in several experiments for the respective strains. The cells had been placed into a chemotaxis chamber at the aggregation-competent stage after 6 h of starvation.

Table I. Motility Parameters of AX2 and cor⁻ *Cells*

Strain	Speed	Turning rate	κ	*n*
	(mm min⁻¹)	*(rad² min⁻¹)*		
Without cAMP gradient				
AX2	7.32 (0.94)	0.879 (0.083)	0.179 (0.035)	11
HG1569	2.33 (0.22)	1.060 (0.201)	0.240 (0.065)	3
HG1570	3.11 (0.63)	1.277 (0.211)	0.260 (0.045)	3
HG1571	4.53 (0.40)	1.107 (0.357)	0.160 (0.087)	3
Average *cor*⁻	3.37 (0.36)	1.115 (0.122)	0.211 (0.036)	9
With cAMP gradient				
AX2	12.37 (0.70)	0.772 (0.056)	0.829 (0.073)	11
HG1569	4.48 (0.80)	0.848 (0.077)	0.465 (0.156)	3
HG1570	5.49 (0.50)	1.057 (0.101)	0.627 (0.097)	3
HG1571	5.73 (0.24)	0.803 (0.096)	0.670 (0.202)	3
Average *cor*⁻	5.10 (0.44)	0.875 (0.055)	0.525 (0.088)	9

Motility parameters are as defined in Fisher at al. (1989). κ, is unitless chemotactic index. *n*, is the number of independent experiments. In each experiment the movements of at least 100 cells were recorded. Average *cor*⁻ represents the average for the three *cor*⁻ strains investigated. The standard errors are shown in parentheses. The mean κ values in the no cAMP controls appear significantly positive because in each experiment there is a small statistically insignificant bias in some random direction that differs in each experiment. The mean κ over many such experiments is artifically greater than zero because it does not reflect the fact that the individual values refer to orientation in a different direction in each experiment. In the measurements with a cAMP gradient the mean direction was close to 0, the direction towards the cAMP source as reported previously for wild-type cells (Fisher et al., 1989).

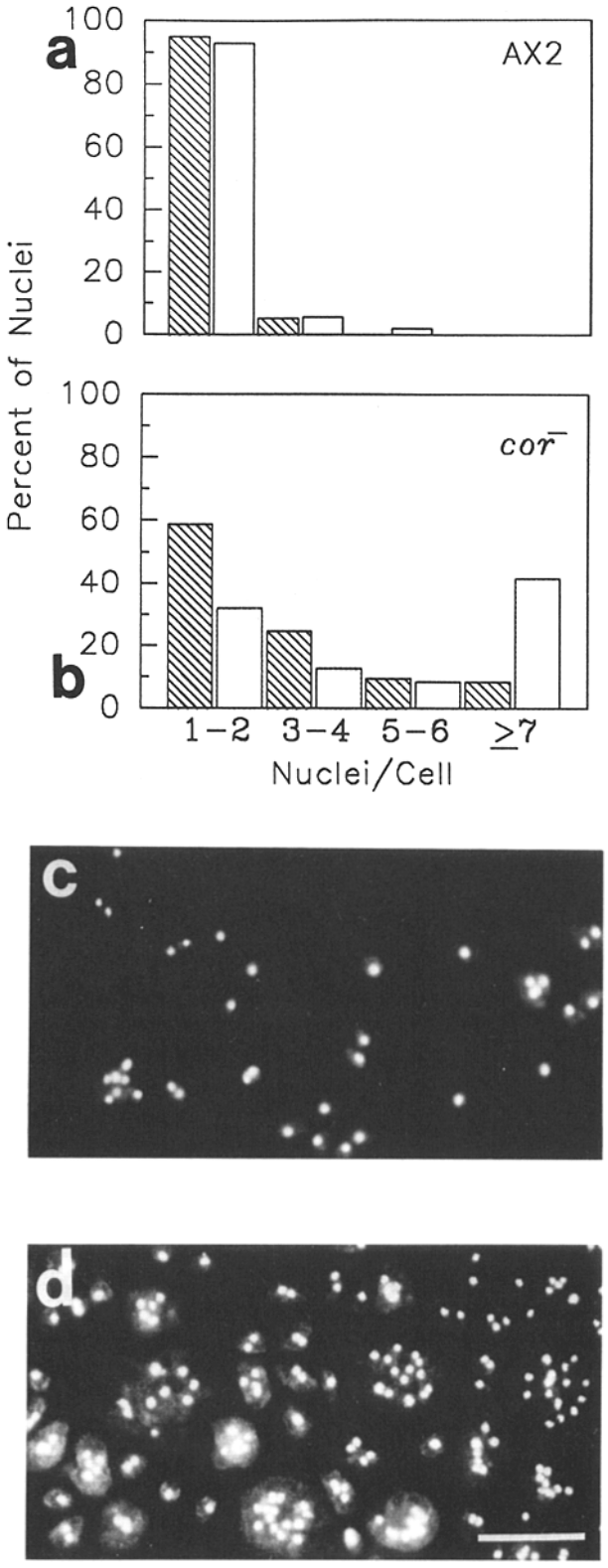

Figure 7. Variation in the number of nuclei in cells axenically grown in suspension or on a glass surface. The histograms refer to wild type (*a*) and to pooled data from *cor*⁻ transformants HG1569, HG1570, and HG1571 (*b*) at the time of transfer from suspension to submerged coverslips (▨) and after 2 d of continued growth on the glass surface (□). (*c*) DAPI-stained nuclei of HG1569 cells from shaken suspension culture and (*d*) of HG1569 cells after 2 d of growth on coverslips. Bar, 50 μm.

which are unable to form a cleavage furrow and to carry-out appropriate cytokinesis (Knecht and Loomis, 1987; De Lozanne and Spudich, 1987). Despite this similarity, *cor*⁻ cells are able to multiply in suspension culture which the myosin null cells can not do. Cytokinesis is, however, not normal in *cor*⁻ cells growing axenically in suspension. By DAPI staining more multinucleate cells were found in the cultures of *cor*⁻ mutants than of the AX2 wild type (Fig. 7, *a* and *b*).

Myosin II null cells can undergo rudimentary cytokinesis by traction-mediated cytofission if they are attached to a substratum (Fukui et al., 1990). In order to examine whether division of *cor*⁻ cells is also facilitated by traction-mediated fission, the numbers of nuclei in cells grown in suspension or attached to a glass surface were compared. Cells grown in suspension culture were transferred onto glass coverslips submerged in the same medium. The distribution of multinucleate cells was determined by DAPI staining immediately and two days after the transfer. While in the suspension cultures of *cor*⁻ strains cells with seven or more nuclei contained 10% of the total number of nuclei, after two days on the glass surface such cells harbored 45% of the nuclei (Fig. 7 *a*). In the wild type the proportion of multinucleate cells increased slightly during growth on glass, but after two days still over 92% of the nuclei were harbored in cells with one or two nuclei and no cells were observed with more than seven nuclei. These results show that in *cor*⁻ mutants, attachment of cells to a surface during axenic growth does not favor cell division, which differs from the behavior of myosin II mutants.

Localization of Coronin in Dividing AX2 Cells

The inefficiency of cytokinesis in *cor*⁻ cells prompted us to investigate the localization of coronin in dividing wild-type cells. AX2 cells were synchronized on glass coverslips submerged in medium, fixed and labeled with anti-coronin antibodies (Fig. 8, *middle*). As a second label either phalloidin, DAPI or anti-myosin antibodies were employed (Fig. 8, *right*). Cells at an early stage of cytokinesis showed a figure-eight staining pattern with both phalloidin and anti-coronin antibodies (Fig. 8 *a*). Both labels were concentrated in the cell cortex of the two emerging daughter cells. This pattern was similar to the phalloidin-labeling pattern that has been reported for cells dividing under pressure applied by an agar overlay (Fukui et al., 1987; Fukui and Inoué, 1991), except that the cleavage furrow was not clearly labeled with phalloidin under our conditions. At later stages of cytokinesis both F-actin and coronin labeling was concentrated at the front of the daughter cells (Fig. 8, *b* and *c*). Thus the peripheral coronin-containing cortical rings of F-actin as seen in Fig. 8 *a* seem to be converted into the cortical network at the anterior edges of the daughter cells in the course of cytokinesis.

The cell shown in Fig. 8 *d* was double labeled with anti-coronin and anti-myosin antibodies after fixation under an agar overlay. As in Fig. 8, *b* and *c* the coronin label is seen to be concentrated at the front of the emerging daughter cells. The cleavage furrow is clearly recognized by an hour-glass shaped accumulation of myosin. This contractile ring is almost free of coronin label.

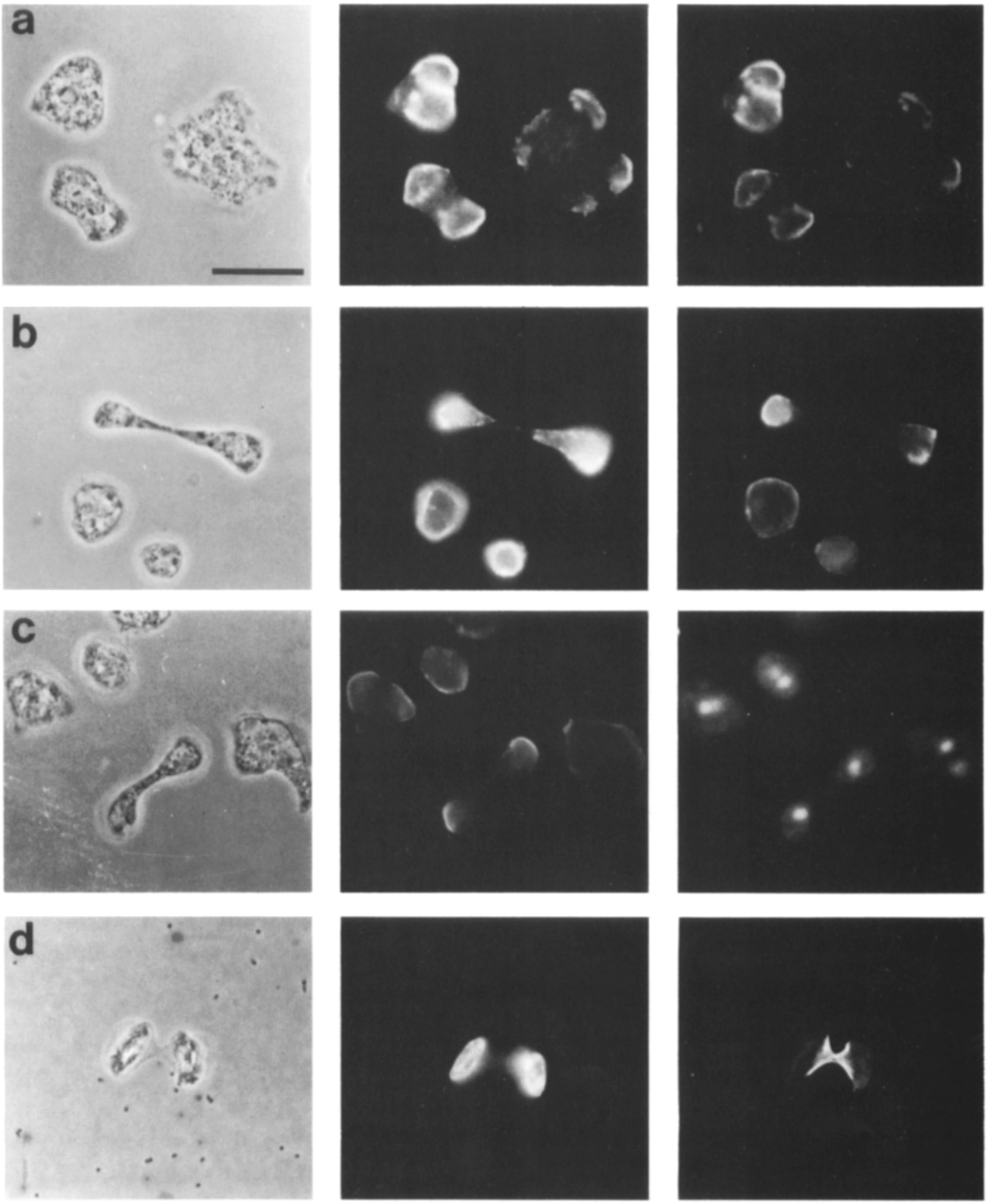

Figure 8. Localization of coronin relative to F-actin and myosin II in dividing AX2 cells. The left panel shows phase-contrast images and the middle panel immunofluorescence labeling of coronin. The right panel shows in *a* and *b* the labeling of F-actin by phalloidin, in *c* the staining of nuclei with DAPI, and in *d* the labeling of myosin II. (*a*) The cell on the left side is at an early stage of cytokinesis. It shows colocalization of coronin and F-actin in a peripheral ring in each of the nascent daughter cells. The cell on the right side shows the typical accumulation of F-actin in cortical projections of non-dividing cells. (*b* and *c*) The dumbbell-shaped cells in late metaphase show the localization of coronin at the front of each of the daughter cells where F-actin is also enriched. (*d*) Coronin is excluded from the cleavage furrow where myosin II is accumulated. For (*a–c*) cells were attached to a glass surface submerged in nutrient medium, for (*d*) the dividing cell was sandwiched by an agar overlay. Bar, 20 μm.

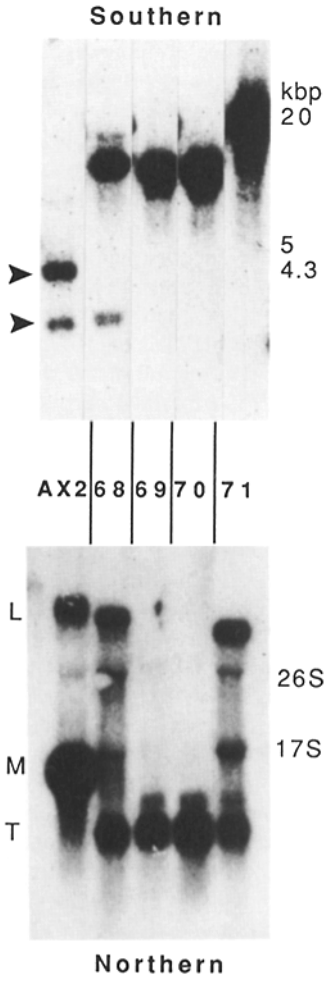

Figure 9. Southern and Northern blots. DNA and RNA were isolated from AX2 and *cor*⁻ mutants designated as in Fig. 4. The blots were hybridized with a probe comprising the entire coding region of a coronin cDNA. (*Top*) Southern blot of genomic DNA restricted with HincII. Markers on the right show sizes in kbp. Arrows on the left indicate positions of the two wild-type DNA fragments detected, which are absent (69, 70, 71) or altered in mobility (68) in the DNA of the mutants. (*Bottom*) Northern blot of total RNA from growth-phase cells. Positions of the 26S and 17S ribosomal RNAs are indicated on the right. On the left are indicated the positions of the minor long (*L*) and major (*M*) coronin transcripts in the wild-type RNA, and the truncated transcript (*T*) in the transformant strains.

Characterization of the Mutants at the DNA Level

DNA was isolated from the four mutant strains and analyzed by Southern blotting and hybridization to a coronin cDNA probe (Fig. 9, *top*). A blot of genomic DNA restricted with HincII showed that in the strains HG1569 and HG1570 the two fragments of 4.1 and 3.2 kbp recognized in wild-type DNA were replaced by a single band of ~10 kbp. This is the size of a fusion between the two wild-type HincII fragments and the antibiotic resistance cassette, the product predicted from the replacement of the native coronin gene with a single engineered construct that lacks a HincII site.

DNA from HG1568 showed a different pattern, in which the smaller fragment was slightly bigger than the 3.2-kbp fragment of the native gene and the larger fragment was longer than the 10-kbp replacement fragment lacking the HincII site. The hybridization pattern of DNA from strain HG1571 showed a single band, but one corresponding to a considerably larger restriction fragment than in any of the other strains.

The results can be interpreted in terms of a clean gene replacement in the case of the HG1569 and HG1570 strains. The hybridization pattern to strain HG1571 DNA was also consistent with the elimination of the native gene by an engineered transforming fragment but through a different recombination event as that experienced by the HG1569 and HG1570 transformants. The larger size of the hybridizing fragment and the greater intensity of the hybridization signal suggests that in HG1571 the replacement of the native gene was accompanied by the integration of multiple copies of the transforming fragment at the coronin locus. The difference observed at the DNA level between this strain and the other two gene replacement mutants may be causally related to its even slower growth rate in axenic suspension culture.

The hybridization pattern to DNA from strain HG1568 can not be explained in terms of gene conversion but possibly as a recombination event leading to the insertion of the engineered copy in tandem into the native copy of the coronin gene. Such a recombination event could permit the restoration of the coronin gene and the observed reversion of the phenotype by deletion of the inserted exogenous copy. The finding that this event takes place even under antibiotic selection could be explained if an additional copy of the antibiotic resistance cassette was inserted elsewhere in the genome, or if revertant nuclei capable of directing the synthesis of coronin could survive as heterokaryons in cells containing *cor*⁻/G418ʳ nuclei. These possibilities remain to be investigated.

Coronin Transcripts in the Mutant Strains

Northern blots of RNA isolated from the wild-type cells showed a major transcript and a larger minor transcript (Fig. 9, *bottom*). All four mutants expressed a truncated coronin transcript at a lower level than that of the major wild-type transcript. In the RNA of strains HG1569 and HG1570 only this truncated transcript was observed. In the RNA from strains HG1568 and HG1571 additional larger transcripts were detectable. They differed in size from each other and also from the minor transcript in AX2 RNA.

The expression of a truncated transcript in the mutants is consistent with the disruption of the *cor*⁻ locus as indicated by Southern hybridization. The truncated transcript is probably the product of transcription starting in the native coronin promoter and terminating in the actin regulatory sequences of the antibiotic resistance cassette. This transcript may be unstable and thus detectable only at a low level. The nature of the minor larger transcript detectable in the wild-type RNA has not been determined. Surprisingly, in the HG1568 strain no coronin transcript of normal length was detectable although it consists of a mixed population of mutant and revertants that produce coronin. It is possible that the aberrant long transcript detected in the RNA from this strain is capable of directing the synthesis of coronin.

Discussion

Phenotypic Changes in Coronin Null Mutants

Elimination by gene replacement of the actin-binding protein coronin has resulted in the following easily recognizable phenotypic changes in the AX2 strain of *D. discoideum*. The mutant cells grow more slowly than the parent strain in bacterial lawns on agar plates as well as in axenic suspension culture in liquid medium. The cells exhibit a deficiency in cytokinesis when growing axenically and they become multinucleate, giving rise to cytoplasmic masses containing sometimes more than 30 nuclei. A causal relationship between lack of coronin and these phenotypic changes is indicated by parallel changes in independent transformants, and

is confirmed by revertants obtained in an unstable transformant. In this transformant, reappearance of coronin is associated with recovery of the wild-type phenotype.

The *cor*⁻ mutants show that coronin is neither essential for actin assembly nor for the normal localization of the actin filaments. The formation of cell-surface extensions called crowns, and multicellular development are also observed in the absence of coronin. While these qualitative data do not exclude a role for coronin in these processes, it is clear that its participation is dispensable under the conditions employed.

Aggregation-competent cells lacking coronin move more slowly than control cells but they are still capable of chemotactic orientation in a cAMP gradient. The chemotactic responsiveness in the absence of coronin is notable because of the sequence relationship of coronin to β-subunits of G proteins. Because of this relationship a function for coronin in regulating the transmission of signals from chemoattractant receptors via G proteins to the actin skeleton has been suggested (de Hostos et al., 1991). The moderate reduction in the accuracy of *cor*⁻ cell orientation in a stable gradient (Table I) would be consistent with a regulatory role of coronin in chemotaxis, and this role may become more obvious under less optimal conditions than have been used. The multiple defects observed in *cor*⁻ mutants indicate, however, that the action of coronin is not specifically linked to chemotactic signal transmission pathways.

Van der Voorn and co-workers (1990) have noted that the repeating sequence motif which is strongly conserved among the Gβ-subunits, and which is seen in coronin (de Hostos et al., 1991), is also present in several other proteins with diverse functions. Among these is the gene product of the CDC4 locus of yeast which has been proposed to be a component of the nuclear skeleton that is required in the triggering of chromosomal duplication at the G1/S-phase boundary of the cell cycle (Yochem and Byers, 1987; Choi et al., 1990). Even if coronin were not involved in signal transduction through G proteins that are coupled to cell-surface receptors, it would remain possible that coronin is linked to Gα-like molecules in signaling circuits. For instance, trimeric G proteins have been reported to be involved in the function of the Golgi apparatus (Burgoyne, 1992; Barr et al., 1992) and have thus been implicated in intracellular signaling pathways.

Coronin and Cell Growth

The retardation of growth observed in *cor*⁻ cells may stem from defects in processes common to cells that take-up bacteria by phagocytosis and liquid nutrients by pinocytosis. Since in both cases the endocytotic vesicles have to pass the cortical actin layer of the cells, it is reasonable to propose that coronin takes part in a process that mediates this passage. Time-lapse movies have shown that in wild-type cells, engulfed bacteria pass the cell cortex slowly before they are carried along with the intracellular particle movement (Gerisch, 1964). Therefore, passage through the cortical actin network may be a rate-limiting step of nutrient uptake in wild-type cells, or may become rate-limiting in the mutants that lack coronin. One possibility is that coronin is involved in the reorganization of the actin network that enables particles to pass. One may extrapolate that coronin is involved whenever restructuring of the actin system is required for rapid shape changes in the highly motile *Dictyostelium* cells.

Involvement of Coronin in Cytokinesis

D. discoideum AX2 cells divide well when growing on bacteria, giving rise almost exclusively to mononucleate cells. During axenic growth a portion of cells containing several nuclei is found, indicating that karyokinesis is not always connected with cytokinesis under these conditions. The lack of coronic markedly enhances this tendency. This effect should be interpreted in terms of the accumulation of coronin in the distal portions of dividing cells. The cleavage furrow is almost depleted of coronin in late mitotic cells. In this furrow myosin II is seen to be enriched when cells are sandwiched between an agar layer and glass (Fukui and Inoué, 1991), and the myosin is needed for contraction of the ring as indicated by the cytokinesis defect in myosin II null mutants (Fukui et al., 1990).

The analysis of myosin II–defective cells has revealed that conventional double-headed myosin is essential for cytokinesis of suspended cells. Cells attached to a substratum can irregularly divide in the absence of myosin II by traction-mediated cytofission. In this process the multiple leading edges which exist in the giant myosin II–defective cells draw pieces of a cell apart from each other, thus giving rise to fragments with irregular numbers of nuclei (Fukui et al., 1990). Taking together that coronin is accumulated at the leading edges of wild-type cells and that motility is reduced in *cor*⁻ cells, it is reasonable to propose that coronin plays a role in the generation or transmission of traction by the microfilament system. It may be assumed that impairment of traction disturbs cytokinesis even in myosin II–containing cells, as it is observed in *cor*⁻ cells attached to a substratum. We can not say which role coronin plays in cytokinesis of suspended cells, but since these cells still divide in the absence of coronin, it is evident that the lack of coronin does not prevent the formation of a cleavage furrow in the way that lack of myosin II does. Structures resembling a cleavage furrow have been found by scanning electron microscopy of mutant cells grown on a substratum (Fig. 5, *c* and *d*).

The inability of *cor*⁻ cells to divide properly under axenic conditions points to a role of coronin in cell division and illustrates that various, probably independent, actin-based mechanisms are involved in guaranteeing proper cytokinesis (Satterwhite and Pollard, 1992). In conclusion, the defects in cell growth, locomotion, and cytokinesis show that coronin is involved in more than a single function of the actin system and suggest that the protein plays a role in the reorganization of this system.

The authors would like to thank Drs. A. Barth, J. Blusch, P. Fisher, and D. Manstein for helpful discussions. M. Ecke, C. Heizer, and U. Masslich provided excellent technical assistance.

This work was supported by a fellowship from the *Alexander von Humboldt Stiftung* to E. de Hostos and grants from the *SFB* 266 of the *Deutsche Forschungsgemeinschaft* and from the *Fonds der Chemischen Industrie* to G. Gerisch.

Received for publication 21 August 1992 and in revised form 28 September 1992.

References

André, E., M. Brink, G. Gerisch, G. Isenberg, A. Noegel, M. Schleicher, J. E. Segall, and E. Wallraff. 1989. A *Dictyostelium* mutant deficient in severin, an F-actin fragmenting protein, shows normal motility and chemotaxis. *J. Cell Biol.* 108:985–995.

Ashworth, J. M., and D. J. Watts. 1970. Metabolism of the cellular slime mould *Dictyostelium discoideum* grown in axenic culture. *Biochem. J.*

119:175–182.
Barr, F. A., A. Leyte, and W. B. Huttner. 1992. Trimeric G proteins and vesicle formation. *Trends Cell Biol.* 2:91–94.
Berlot, C. H., J. A. Spudich, and P. N. Devreotes. 1985. Chemoattractant-elicited increases in myosin phosphorylation in *Dictyostelium*. *Cell.* 43: 307–314.
Bomblies, L., E. Biegelmann, V. Döring, G. Gerisch, H. Krafft-Czepa, A. A. Noegel, M. Schleicher, and B. M. Humbel. 1990. Membrane-enclosed crystals in *Dictyostelium discoideum* cells consisting of developmentally regulated proteins with sequence similarities to known esterases. *J. Cell Biol.* 110:669–679.
Brink, M., G. Gerisch, G. Isenberg, A. A. Noegel, J. E. Segall, E. Wallraff, and M. Schleicher. 1990. A *Dictyostelium* mutant lacking an F-actin cross-linking protein, the 120 kD gelation factor. *J. Cell Biol.* 111:1477–1489.
Burgoyne, R. D. 1992. Trimeric G proteins in Golgi transport. *Trends Biochem. Sci.* 17:37–88.
Choi, W.-J., M. W. Clark, J. X. Chen, and A. Y. Jong. 1990. The *CDC4* gene product is associated with the yeast nuclear skeleton. *Biochem. Res. Commun.* 172:1324–1330.
Claviez, M., K. Pagh, H. Maruta, W. Baltes, P. Fisher, and G. Gerisch. 1982. Electron microscopic mapping of monoclonal antibodies on the tail region of *Dictyostelium* myosin. *EMBO (Eur. Mol. Biol. Organ.) J.* 1:1017–1022.
Cox, D., J. Condeelis, D. Wessels, D. Soll, H. Kern, and D. A. Knecht. 1992. Targeted disruption of the ABP-120 gene leads to cells with altered motility. *J. Cell Biol.* 116:943–955.
Cunningham, C. C., T. P. Stossel, and D. J. Kwiatkowski. 1991. Enhanced motility in NIH 3T3 fibroblasts that overexpress gelsolin. *Science (Wash. DC).* 251:1233–1236.
Cunningham, C. C., J. B. Gorlin, D. J. Kwiatkowski, J. H. Hartwig, P. A. Janmey, H. R. Byers, and T. P. Stossel. 1992. Actin-binding protein requirement for cortical stability and efficient locomotion. *Science (Wash. DC).* 255:325–327.
de Hostos, E. L., B. Bradtke, F. Lottspeich, R. Guggenheim, and G. Gerisch. 1991. Coronin, an actin-binding protein of *Dictyostelium discoideum* localized to cell surface projections, has sequence similarities to G protein β subunits. *EMBO (Eur. Mol. Biol. Organ.) J.* 10:4097–4104.
De Lozanne, A., and J. A. Spudich. 1987. Disruption of the *Dictyostelium* myosin heavy chain gene by homologous recombination. *Science (Wash. DC).* 236:1086–1091.
Devreotes, P. N., and S. H. Zigmond. 1988. Chemotaxis in eukaryotic cells: a focus on leukocytes and *Dictyostelium*. *Ann. Rev. Cell Biol.* 4:649–686.
Feinberg, A. P., and B. Vogelstein. 1983. A technique for radiolabeling DNA restriction endonuclease fragments to high specific activity. *Anal. Biochem.* 132:6–13.
Fisher, P. R., E. Smith, and K. L. Williams. 1981. An extracellular chemical signal controlling phototactic behavior in *D. discoideum* slugs. *Cell.* 23: 799–807.
Fisher, P. R., W. N. Grant, U. Dohrmann, and K. L. Williams. 1983. Spontaneous turning behaviour by *Dictyostelium discoideum* slugs. *J. Cell Sci.* 62:161–170.
Fisher, P. R., R. Merkl, and G. Gerisch. 1989. Quantitative analysis of cell motility and chemotaxis in *Dictyostelium discoideum* by using an image processing system and a novel chemotaxis chamber providing stationary chemical gradients. *J. Cell Biol.* 108:973–984.
Fukui, Y., and S. Inoué. 1991. Cell division in *Dictyostelium* with special emphasis on actomyosin organization in cytokinesis. *Cell Motil. Cytoskeleton.* 18:41–54.
Fukui, Y., S. Yumura, and T. K. Yumura. 1987. Agar-overlay immunofluorescence: high-resolution studies of cytoskeletal components and their changes during chemotaxis. *Methods Cell Biol.* 28:347–356.
Fukui, Y., A. De Lozanne, and J. A. Spudich. 1990. Structure and function of the cytoskeleton of a *Dictyostelium* myosin-defective mutant. *J. Cell Biol.* 110:367–378.
Gerisch, G. 1964. *Dictyostelium purpureum* (Acrasina), Vermehrungsphase (Film E629/1963). *In* Encyclopedia Cinematographica. G. Wolf, editor. Institut für den Wissenschaftlichen Film, Göttingen, Germany.
Gerisch, G., A. A. Noegel, and M. Schleicher. 1991. Genetic alteration of proteins in actin-based motility systems. *Ann. Rev. Physiol.* 53:607–628.
Harlow, E., and D. Lane. 1988. Antibodies. Cold Spring Harbor Laboratory, Cold Spring Harbor, NY. 726 pp.
Jay, P. Y., and E. L. Elson. 1992. Surface particle transport mechanism independent of myosin II in *Dictyostelium*. *Nature (Lond.).* 356:438–440.
Jung, G., and J. A. Hammer III. 1990. Generation and characterization of *Dictyostelium* cells deficient in a myosin I heavy chain isoform. *J. Cell Biol.* 110:1955–1964.
Knecht, D. A., and W. F. Loomis. 1987. Antisense RNA inactivation of myosin heavy chain gene expression in *Dictyostelium discoideum*. *Science (Wash. DC).* 236:1081–1086.
Knecht, D. A., S. M. Cohen, W. F. Loomis, and H. F. Lodish. 1986. Developmental regulation of *Dictyostelium discoideum* actin gene fusions carried on low-copy and high-copy transformation vectors. *Mol. Cell. Biol.* 6:3973–3983.
Laemmli, U. K. 1970. Cleavage of structural proteins during the assembly of the head of bacteriophage T4. *Nature (Lond.).* 227:680–685.
Manstein, D. J., M. A. Titus, A. De Lozanne, and J. A. Spudich. 1989. Gene replacement in *Dictyostelium*: generation of myosin null mutants. *EMBO (Eur. Mol. Biol. Organ.) J.* 8:923–932.
Mehdy, M. C., D. Ratner, and R. A. Firtel. 1983. Induction and modulation of cell-type-specific gene expression in *Dictyostelium*. *Cell.* 32:763–771.
Noegel, A. A., and M. Schleicher. 1991. Phenotypes of cells with cytoskeletal mutations. *Curr. Opin. Cell Biol.* 3:18–26.
Pollard, T. D., and J. A. Cooper. 1986. Actin and actin-binding proteins: a critical evaluation of mechanisms and functions. *Ann. Rev. Biochem.* 55:987–1035.
Satterwhite, L. L., and T. D. Pollard. 1992. Cytokinesis. *Curr. Opin. Cell Biol.* 4:43–52.
Schleicher, M., and A. A. Noegel. 1992. Dynamics of the *Dictyostelium* cytoskeleton during chemotaxis. *New Biologist.* 4:461–472.
Segall, J. E., P. R. Fisher, and G. Gerisch. 1987. Selection of chemotaxis mutants of *Dictyostelium discoideum*. *J. Cell Biol.* 104:151–161.
Titus, M. A., H. M. Warrick, and J. A. Spudich. 1989. Multiple actin-based motor genes in *Dictyostelium*. *Cell Regul.* 1:55–63.
van der Voorn, L., M. Gebbink, R. H. A. Plasterk, and H. L. Ploegh. 1990. Characterization of a G-protein β-subunit gene from the nematode *Caenorhabditis elegans*. *J. Mol. Biol.* 213:17–26.
Waddell, D. R., K. Duffy, and G. Vogel. 1987. Cytokinesis is defective in *Dictyostelium* mutants with altered phagocytic recognition, adhesion, and vegetative cell cohesion properties. *J. Cell Biol.* 105:2293–2300.
Wallraff, E., M. Schleicher, M. Modersitzki, D. Rieger, G. Isenberg, and G. Gerisch. 1986. Selection of *Dictyostelium* mutants defective in cytoskeletal proteins: use of an antibody that binds to the ends of α-actinin rods. *EMBO (Eur. Mol. Biol. Organ.) J.* 5:61–67.
Wessels, D., and D. R. Soll. 1990. Myosin II heavy chain null mutant of *Dictyostelium* exhibits defective intracellular particle movement. *J. Cell Biol.* 111:1137–1148.
Wessels, D., D. R. Soll, D. Knecht, W. F. Loomis, A. De Lozanne, and J. A. Spudich. 1988. Cell motility and chemotaxis in *Dictyostelium* amebae lacking myosin heavy chain. *Dev. Biol.* 128:164–177.
Witke, W., W. Nellen, and A. Noegel. 1987. Homologous recombination in the *Dictyostelium* α-actinin gene leads to an altered mRNA and lack of the protein. *EMBO (Eur. Mol. Biol. Organ.) J.* 6:4143–4148.
Witke, W., M. Schleicher, and A. A. Noegel. 1992. Redundancy in the microfilament system: abnormal development of *Dictyostelium* cells lacking two F-actin cross-linking proteins. *Cell.* 68:53–62.
Yochem, J., and B. Byers. 1987. Structural comparison of the yeast cell division cycle gene *CDC4* and a related pseudogene. *J. Mol. Biol.* 195:233–245.